LIMNOLOGY and OCEANOGRAPHY

ASLO

Limnol. Oceanogr. 64, 2019, 982–995

doi: 10.1002/lno.11089

Microbial oxidation of nitrogen supplied as selected organic nitrogen compounds in the South Atlantic Bight

Julian Damashek,[1] **Bradley B. Tolar**,[1,a] **Qian Liu**,[1,b] **Aimee O. Okotie-Oyekan**,[1] **Natalie J. Wallsgrove**,[2] **Brian N. Popp**,[2] **James T. Hollibaugh**[*1]

[1]Department of Marine Sciences, University of Georgia, Athens, Georgia
[2]Department of Earth Sciences, University of Hawai'i at Manoa, Honolulu, Hawaii

Abstract

Dissolved organic nitrogen (DON) can account for a large fraction of the dissolved nitrogen (N) pool in the ocean, but the cycling of marine DON is poorly understood. Recent discoveries that urea- and cyanate-N can be oxidized by some strains of Thaumarchaeota suggest that these abundant microbes may be able to access and oxidize a fraction of the DON pool. However, measurements of the oxidation of N supplied as DON compounds are scarce. Here, we compare oxidation rates of N supplied as a variety of DON compounds in samples from Georgia coastal waters, where nitrifier communities are numerically dominated by Thaumarchaeota. Our data indicate that polyamine-N is particularly amenable to oxidation compared to the other DON compounds tested. Oxidation of N supplied as putrescine (1,4-diaminobutane) was generally higher than that of N supplied as glutamate, arginine, or urea, and was consistently 5–10% of the ammonia oxidation rate. Our data also suggest that the oxidation rate of polyamine-N may increase as the length of the carbon skeleton increases. Oxidation of N supplied as putrescine, urea, and glutamate were all highest near the coast and lower further offshore, consistent with patterns of ammonia oxidation in these waters. Though it is unclear whether oxidation of polyamine-N reflects direct oxidation by Thaumarchaeota or combines remineralization and subsequent ammonia oxidation, more rapid oxidation of N from putrescine compared to amino acids or urea suggests that polyamine-N may contribute significantly to nitrification in the ocean.

Dissolved organic nitrogen (DON) is a complex of compounds that accounts for a substantial fraction of the nitrogen (N) pool in the coastal ocean (Sipler and Bronk 2015). Relatively little is known about the biogeochemical cycling of DON compared to that of dissolved inorganic nitrogen (predominately ammonium, nitrite, and nitrate). Recent reports show that some cultivated Thaumarchaeota can grow by oxidizing the N in urea (Tourna et al. 2011; Bayer et al. 2016; Qin et al. 2017; Carini et al. 2018) or cyanate (Palatinszky et al. 2015), that Thaumarchaeota in the coastal Arctic Ocean can assimilate significant amounts of urea-N into DNA (Connelly et al. 2014), and that thaumarchaeal *ureC* genes are present in many ocean basins (Yakimov et al. 2011; Alonso-Sáez et al. 2012; Smith et al. 2016; Tolar et al. 2017). These observations suggest that some organic N compounds can be oxidized by nitrifiers, verified by recent measurements of the contribution of urea-derived N to nitrification in several Thaumarchaeota-dominated nitrifier communities (Tolar et al. 2017). Oxidation of urea- and cyanate-N likely proceeds by reactions yielding free ammonium (NH_4^+), which begs the question of whether DON compounds with different chemical structures (e.g., amines, α-amino groups, etc.) are also directly available for oxidation by nitrifiers, including Thaumarchaeota, or whether regeneration to ammonium is an essential first step in the oxidation of marine DON.

Polyamines are primary amines that consist of an aliphatic hydrocarbon backbone with two or more amine substitutions. They are ubiquitous in eukaryotic and prokaryotic cells where they participate in integral cellular processes such as nucleic acid synthesis and stabilization, biosilica precipitation in diatoms, and protein synthesis (Kröger et al. 2000; Iacomino et al. 2012). Polyamines

*Correspondence: aquadoc@uga.edu

[a]Present address: Department of Earth System Science, Stanford University, Stanford, California

[b]Present address: Key Laboratory of Marine Ecosystem and Biogeochemistry, Second Institute of Oceanography, State Oceanic Administration, Hangzhou, Zhejiang, China

Author Contribution Statement: JD, BBT, QL, BNP, and JTH designed the research. JD, BBT, QL, and JTH conducted the field work. JD, BBT, QL, and AOO-O extracted DNA and performed the qPCR analyses. BBT, NJW, and BNP performed ^{15}N analyses. JD analyzed the data. JD and JTH wrote the paper, with input from all other coauthors.

Additional Supporting Information may be found in the online version of this article.

are present at millimolar concentrations in phytoplankton and bacterial cells (e.g., Tabor and Tabor 1985; Nishibori and Nishijima 2004; Liu et al. 2016), but their standing stocks in aquatic environments are in the low nanomolar or picomolar range, suggesting rapid biogeochemical cycling (Nishibori et al. 2001*a*,*b*; Lu et al. 2014; Liu et al. 2015; Krempaska et al. 2018). Recent work has expanded our understanding of polyamine assimilation and the cycling of polyamine carbon (C) in aquatic systems (e.g., Poretsky et al. 2010; Mou et al. 2011, 2015; Liu et al. 2015; Lu et al. 2015; Krempaska et al. 2018), but little is known about the fate of polyamine-N. Although polyamines represent a small fraction of the marine DON pool, high-turnover rates (comparable to dissolved free amino acids [DFAA]) suggest they may account for a large fraction of microbial DON cycling in the ocean. Much of the polyamine-C in the coastal ocean is respired by heterotrophs (Höfle 1984; Liu et al. 2015), which should provide a significant source of regenerated ammonium available for nitrification. Yet, oxidation rates of polyamine-N have not previously been measured in the ocean, leaving open a significant question about their role in the marine N cycle. There is genomic evidence that Thaumarchaeota, the dominant marine ammonia oxidizer, may be capable of polyamine synthesis and/or assimilation: many thaumarchaeal genomes encode genes involved in polyamine synthesis, and a recent freshwater isolate also contains putative *potABCD* genes, which encode polyamine transporters in many bacteria (Sauder et al. 2018). Although the presence of these genes suggests polyamines have an important biochemical role in thaumarchaeal cells, the availability of polyamine-N for oxidation by Thaumarchaeota or nitrifying bacteria has not been tested: to our knowledge, oxidation rates of polyamine-N have not been reported from any field environments or isolates.

Previous work in the South Atlantic Bight (SAB) demonstrated a correlation between Thaumarchaeota abundance and ammonia oxidation rates, with highest rates at inshore stations and a subsurface maxima near the shelf-break (Tolar et al. 2017; Liu et al. 2018). Ammonia-oxidizing communities in the SAB are composed predominantly of Thaumarchaeota, but with important geographic differences in phylogenetic identity (Liu et al. 2018). Thaumarchaeal populations in inshore waters around Sapelo Island are similar to the strain *Nitrosopumilus maritimus* SCM1 (16S, 99.4–99.6%; *amoA*, 91.2–98.8% nucleotide identity) and display a strong seasonal cycle of abundance, increasing > 3 orders of magnitude in the summer to dominate the ammonia-oxidizing microbial population (Hollibaugh et al. 2011, 2014; Whitby et al. 2017; Liu et al. 2018). Thaumarchaeota populations in shallow nearshore waters over the continental shelf show high diversity, including *Nitrosopumilus*-like, *Nitrosoarchaeum*-like, and group 1.1b Archaea (Liu et al. 2018). Abundance fluctuates seasonally, similar to the inshore population. Thaumarchaeota populations in deeper outer shelf and shelf-break waters are primarily from the marine clades "Water Column A" (WCA) and "Water Column B" (WCB), considered shallow- and deep-water ecotypes, respectively (Francis et al. 2005; Beman et al. 2008). There is less seasonal variability at these offshore locations (Liu et al. 2018).

Here, we compare the oxidation rates of N supplied as ammonium, urea, selected amino acids, and selected polyamines across the SAB. This data set allows us to assess the contribution of polyamine-N to nitrification by nitrifier assemblages dominated by a range of Thaumarchaeota ecotypes. Our data suggest that N supplied as polyamines is oxidized rapidly in the ocean, largely outstripping oxidation rates of N from the other DON compounds tested, but also indicate that ammonium is the predominant substrate for nitrification in the SAB.

Methods

Field sampling and nutrient analysis

Samples were collected from four regions (inshore, mid-shelf, shelf-break, and oceanic) of the SAB off the Georgia (U.S.A.) coast (Fig. 1; Supporting Information Table S1), with terminology modified from Liu et al. (2018) as follows. "Inshore" stations were within the barrier island complex. "Mid-shelf" stations were outside the barrier island complex to depths < 40 m; due to limited sampling in this zone, no demarcation between "mid-shelf" and "nearshore" stations (as in Liu et al. 2018) was made. "Shelf-break" stations were between 40 m and 500 m depth. While Liu et al. (2018) did not sample waters past the shelf-break, we included deeper stations further offshore (bottom depth > 500 m), which are designated "oceanic" stations. Note that the maximum depth sampled was ≤ 500 m due to equipment limitations.

Inshore samples were collected from a dock at Marsh Landing on the Duplin River (Sapelo Island) and the dock at the Skidaway Institute of Oceanography (Fig. 1). Both inshore sites are salt marsh-dominated estuaries. Water from both sites was sampled from a depth ≤ 1 m and was processed immediately at a nearby laboratory (the University of Georgia Marine Institute on Sapelo Island or onboard the R/V *Savannah*). Water quality data for Marsh Landing samples were collected as part of the Sapelo Island National Estuarine Research Reserve monitoring program. Relevant data from the Lower Duplin ("LD") sonde were downloaded from NOAA/CDMO (http://cdmo.baruch.sc.edu/aqs/, last accessed 22 May 2018).

Most SAB samples were collected in August 2017 on the R/V *Savannah* (cruise SAV-17-16) along transects across the continental shelf and the Gulf Stream and into the western Sargasso Sea, with sampling focused around the shelf-break (Fig. 1). Water from multiple depths was collected using 12-liter Niskin bottles mounted on a rosette equipped with a Sea-Bird SBE25 CTD. Profiles of salinity, temperature, dissolved oxygen, fluorescence, and photosynthetically active radiation (PAR) were collected using the CTD system as described previously (Liu et al. 2018). PAR attenuation (K_d) was calculated from plots of ln(PAR) vs. depth as in Liu et al. (2018).

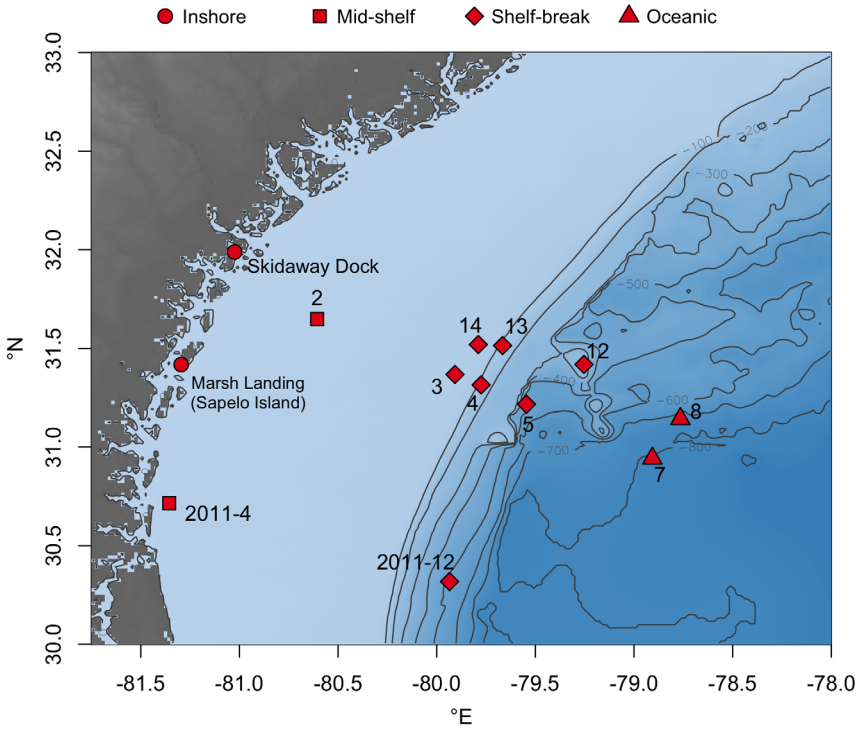

Fig. 1. Sampling area near the Georgia coast. Shape indicates the designated region. Gray lines are 100 m depth contours, and blue shading indicates water depth from shallow (light) to deep (dark).

Two additional SAB stations were sampled in October 2011 (described previously by Liu et al. 2015 and Tolar et al. 2017) and are referred to as "2011-4" and "2011-12" (Fig. 1). Environmental data and some of the microbial and rate data from 2011 stations are available in other publications (Liu et al. 2015; Tolar et al. 2017; *see* Supporting Information Table S1).

Nutrient samples were filtered through 0.22 μm pore size Durapore GVWP filters (Millipore Sigma) and frozen at −20°C immediately after collection, then stored at −80°C until analysis. Dissolved nitrate (NO_3^-), nitrite (NO_2^-), phosphate (PO_4^{3-}), and silicate (SiO_4^{4-}) were measured using a Bran and Luebbe AA3 autoanalyzer as described previously (Wilkerson et al. 2015). Ammonium and urea were measured manually using the phenolhypochlorite method (Solórzano 1969) and the diacetylmonoxime method (Rahmatullah and Boyde 1980; Mulvenna and Savidge 1992), respectively.

Oxidation rate measurements

We used ^{15}N-labeled substrates (98–99% ^{15}N, Cambridge Isotope Laboratories) to measure the oxidation of N supplied as NH_4^+, urea, 1,2-diaminoethane (DAE), 1,3-diaminopropane (DAP), 1,4-diaminobutane (putrescine, PUT), L-glutamic acid (GLU), and L-arginine (ARG). ^{15}N oxidation from NH_4^+, urea, PUT, and GLU were measured extensively, whereas ^{15}N oxidation from DAE, DAP, and ARG was only measured at a subset of stations (Supporting Information Table S1). GLU and ARG were included as a control for remineralization, as their central roles in microbial metabolism leads to rapid catabolism and NH_4^+ regeneration (Hollibaugh 1978; Goldman et al. 1987). PUT was used in routine assessments of the oxidation of polyamine-N because it is one of the most consistently detected polyamines in seawater (Nishibori et al. 2001*a*, 2003; Lu et al. 2014; Liu et al. 2015). Although spermine and spermidine are also common in seawater, ^{15}N-labeled stocks of these polyamines were not commercially available. We measured the oxidation of N from DAE and DAP to investigate the effect of aliphatic chain length (which affects pK_a) on oxidation rate.

Duplicate seawater samples contained in 1-liter polycarbonate or 250 mL high density polyethylene (HDPE) bottles wrapped with aluminum foil (to exclude light) were amended with 10–50 nM ^{15}N-labeled substrate. Marsh Landing samples were then placed in an incubator held at in situ temperature in the dark. Samples taken at the Skidaway dock were placed in a mesh bag and immersed at the sea surface at the sampling site. Samples collected at sea were incubated in a tank of flowing surface seawater or in an incubator held at 18°C in the dark. Incubation bottles were sampled for ^{15}N analysis immediately after substrate addition and again after a period of ~ 24 h. ^{15}N samples were subsampled into 50 mL polypropylene centrifuge tubes, frozen at −20°C, and stored at −80°C until analysis. The $^{15}N/^{14}N$ ratios of the NO_3^- plus NO_2^- (NO_X) pools ($\delta^{15}N_{NOx}$) in the samples were measured using the bacterial denitrifier method to convert NO_X to nitrous oxide (N_2O; Sigman et al. 2001). The $\delta^{15}N$ values of the N_2O produced were measured using a Finnigan MAT-252 isotope ratio mass spectrometer coupled with a modified GasBench

II interface (Casciotti et al. 2002; Beman et al. 2011; McIlvin and Casciotti 2011). Oxidation rates were calculated using an endpoint model (Beman et al. 2011; Damashek et al. 2016). Since the substrates used were uniformly labeled with ^{15}N, the amount of the N added as the ^{15}N spike (in μM) was multiplied by the number of moles of ^{15}N per mole of substrate, which assumes that all of the N atoms have equal probability of being oxidized. This is likely true for urea, DAE, DAP, and PUT, which are symmetrical molecules, but not likely to be true for ARG, which contains 4 N atoms (one in the α-amino position and three in the guanidine structure of its R-group). Abiotic oxidation of organic N was assessed by measuring $^{15}NO_X$ production following ^{15}N amendment and incubation of 0.22 μm filtered seawater (as described above), and potential metabolism of DON by the denitrifying bacteria used to convert NO_X to N_2O was checked by adding ^{15}N-labeled substrates into the bacterial cultures prior to mass spectrometry.

We were unable to measure the in situ concentrations of the individual components of DON used in oxidation experiments, other than urea. Based on previous measurements made in the SAB (Lu et al. 2014; Liu et al. 2015), we assumed concentrations of 1 nM and 0.25 nM for DAE, DAP and PUT, and 10 nM and 5 nM for GLU and ARG, at inshore and mid-shelf/shelf-break/oceanic stations, respectively. Rates of polyamine and amino acid oxidation reported below should therefore be considered potential rates, as amendments as low as 10–50 nM are likely to increase substrate concentrations substantially above in situ. Initial substrate ^{15}N activity was calculated using isotope mass balance using the known concentration and ^{15}N activity of the labeled substrates added and assuming the concentrations described above and natural abundance ^{15}N activity (i.e., 0.3663 atom% ^{15}N).

Microbial communities

Microbial biomass was collected by vacuum filtering 0.5–1.0 L of seawater through a 45 mm diameter, 0.22 μm pore size GVWP Durapore filter (Millipore Sigma), which was immediately immersed in 1.8 mL of lysis buffer (Ferrari and Hollibaugh 1999) in a 5 mL Axygen screw-cap tube (Corning Life Sciences) and frozen at −80°C or on liquid N_2. DNA was extracted following previously published protocols (Ferrari and Hollibaugh 1999; Tolar et al. 2013). Briefly, cells were lysed using lysozyme (1.0 mg mL^{-1}), proteinase K (0.5 mg mL^{-1}), and sodium dodecyl sulfate (SDS) (1%). DNA was purified from lysate using sequential extractions of phenol : chloroform : isoamyl alcohol, chloroform : isoamyl alcohol, and butanol, then mixed with 1 mL Tris-Ethylenediaminetetraacetic acid (TE) (pH 8) and concentrated in an Amicon Ultra-4 centrifugal filter (Millipore Sigma).

Gene abundances were determined using quantitative polymerase chain reaction (qPCR) assays. Details of primers, assay conditions, and amplification efficiencies are given in Supporting Information Table S2. Bacterial, thaumarchaeal, and *Nitrospina* 16S ribosomal RNA (rRNA) genes were quantified as described previously (Mincer et al. 2007; Kalanetra et al. 2009; Tolar et al. 2013). Thaumarchaeal *amoA* abundance was determined using WCA and WCB ecotype assays (Mosier and Francis 2011). All reactions (25 μL total volume) were run in triplicate on a C1000 Touch Thermal Cycler equipped with a CFX96 Real-Time System (Bio-Rad), using either the iTaq Universal Green SYBR Mix (Bio-Rad) or the Platinum qPCR SuperMix-UDG (Thermo Fisher). Standard curves consisted of a dilution series of linearized plasmids from previously sequenced clones. All standard curves had $r^2 \geq 0.99$, and efficiencies for most assays were close to 100% with the exception of *Nitrospina* 16S, which had an average efficiency of 92.9% (Supporting Information Table S2). Since previous studies consistently found far greater abundance of Thaumarchaeota than ammonia-oxidizing bacteria throughout the SAB (Hollibaugh et al. 2011, 2014; Tolar et al. 2017; Liu et al. 2018), we did not quantify ammonia-oxidizing bacteria.

Data analysis

Statistical tests were conducted using R (R Core Team 2015). Pairwise relationships between variables were assessed using Spearman's rank correlation coefficient (Spearman's ρ). If Spearman's ρ indicated a significant correlation, both variables (or transformations of variables) were normally distributed, and scatterplots suggested a linear relationship, model II linear regressions were conducted using the lmodel2 package (Legendre and Legendre 2012; Legendre 2018). Model II regressions were used since both variables in all regressions were random and therefore incorporated measurement error. When log-transformed variables were used in a regression, parameters were calculated using major axis regression, in which the regression line is the first principle component of the scatterplot (Legendre and Legendre 2012). The p value of the regression slope was calculated using 999 permutation tests.

Statistical differences between regions (inshore, shelf-break, and oceanic; Fig. 1) were tested using one-way ANOVA tests. Mid-shelf samples were not included since only two samples were obtained from this region. Similarly, if a region had fewer than three measurements for a variable (e.g., some oxidation rates at inshore stations), this region was not included. Data distributions were assessed using histograms, with log-transformations used to improve normality when necessary. When ANOVA results were significant, a post-hoc Tukey's honest significant difference (HSD) test was conducted using the agricolae package (de Mendiburu 2015) to determine which groups differed from others. When only two regions were compared, a two-tailed t-test was used. To guard against potential bias from unequal numbers of observations between compared groups and the relatively small overall sample size, we compared results of ANOVAs and t-tests to results of corresponding nonparametric tests (the Kruskal-Wallis H test and Mann–Whitney U test, respectively; Legendre and Legendre 2012). Plots were made using the ggplot2 and lemon packages (Wickham 2009; Edwards 2018), and sampling locations were mapped using the marmap package (Pante and Simon-Bouhet 2013).

Table 1. Regional ranges and averages (± SD) of (untransformed) oxidation rates of ^{15}N supplied as ammonium, putrescine, urea, and glutamate. Data for each substrate were log-transformed prior to statistical tests, and regions with $n < 3$ were not included in statistical tests.

	Ammonia oxidation				^{15}N oxidation from putrescine			
Region	***n***	**Range**	**Avg. ± SD**	**Group[a]**	***n***	**Range**	**Avg. ± SD**	**Group[a]**
Inshore	3	121.40–431.00	273.85 ± 154.85	A	3	4.53–84.67	43.79 ± 40.09	A
Mid-shelf	1	86.35			1	33.66		
Shelf-break	10	4.04–229.28	66.22 ± 82.54	A	10	0.22–18.86	7.48 ± 6.84	A
Oceanic	4	0.30–9.55	4.05 ± 3.99	B	4	0.01–0.40	0.18 ± 0.17	B
		$F_{2,14} = 8.8$, $p = 0.003$				$F_{2,14} = 10.6$, $p = 0.002$		
	^{15}N oxidation from urea				^{15}N oxidation from GLU			
	n	**Range**	**Avg. ± SD**	**Group[a]**	***n***	**Range**	**Avg. ± SD**	**Group[a]**
Inshore	2	20.31–62.53			2	1.42–16.78		
Mid-shelf	1	47.52			0			
Shelf-break	10	0.02–8.08	2.67 ± 2.62		7	0.01–1.36	0.77 ± 0.56	
Oceanic	5	0.05–1.17	0.43 ± 0.43		4	0.01–0.40	0.11 ± 0.19	
		$t = 2.1$, $p = 0.057$, df = 11				$t = 2.2$, $p = 0.065$, df = 7		

[a]Statistical groups (capital letters) indicate results of Tukey's HSD test for substrates where an ANOVA indicated significant differences between regions ($p < 0.05$).

Results

Oceanographic conditions, August 2017

Surface-water temperature was relatively constant, ranging from 28.4°C to 31.3°C in samples taken from ≤ 5 m depth. Shelf-break and oceanic samples showed evidence of density stratification, with temperature decreasing with depth and salinity increasing to ~ 50–100 m and then decreasing at greater depths (Supporting Information Table S1, Fig. S1a,b). Dissolved oxygen generally decreased with depth, with minima at 250–350 m near the shelf-break (< 5.0 mg L^{-1}; Supporting Information Fig. S1c, Table S1). Chlorophyll fluorescence exhibited subsurface peaks, particularly near the shelf-break and in some inshore samples (Supporting Information Fig. S1d, Table S1).

Silicate, phosphate, and NO_3^- all increased with depth (Supporting Information Fig. S1e,f,i). The highest concentrations of NO_3^- (> 22.0 μM), phosphate (> 1.5 μM), and silicate (> 11.0 μM, excluding the Skidaway dock sample) were in near-bottom waters at the shelf-break (Sta. 5 and 12; Supporting Information Table S1). While NH_4^+ and NO_2^- displayed almost no overall trend with depth, most oceanic and shelf-break stations had subsurface maxima for these nutrients (Supporting Information Fig. S1g,j, Table S1). Late summer inshore samples had extremely high NO_2^- (3.7 μM and 5.1 μM), and bottom waters at some shelf-break stations also had high NO_2^- (0.5 μM and 0.7 μM, respectively; Supporting Information Table S1). Urea concentrations were low (most < 0.5 μM) and showed no discernible pattern with location or depth (Supporting Information Fig. S1h), though numerous shelf-break stations had subsurface urea maxima of ~ 0.2–0.3 μM (Supporting Information Table S1).

Rate measurements

Rates of NH_4^+ oxidation across Georgia coastal waters ranged from 0.3 nM L^{-1} d^{-1} (Sta. 7, 336 m) to 431.0 nM L^{-1} d^{-1} (Skidaway dock). Maximum oxidation rates of N supplied as other compounds were lower (Table 1; note that rates for polyamines and amino acids are likely potential rates). Oxidation rates of N supplied as PUT were typically higher than rates for N supplied as urea or GLU. Oxidation rates of N in DON compounds were usually less than the NH_4^+ oxidation rate in the same sample. The exceptions were oxidation of PUT-N at Sta. 2011-12 and oxidation of urea N at Sta. 7 (336 m), where the calculated rates were ~ 2.5-fold and ~ 1.2-fold greater than the rate of NH_4^+ oxidation in the same samples, respectively (Supporting Information Table S1).

The highest values for oxidation of N supplied as NH_4^+, PUT, GLU, and urea were all from inshore waters (Table 1). Oxidation rates of NH_4^+ and PUT-N in inshore and shelf-break samples were significantly greater than in oceanic samples (NH_4^+: $F_{2,14} = 8.8$, $p = 0.003$; PUT: $F_{2,14} = 10.6$, $p = 0.002$), while oxidation rates of urea-N and GLU-N were not significantly different between shelf-break and oceanic samples (Table 1). Results from parametric and nonparametric tests were consistent with the exception of urea-N oxidation rates, which were significantly different in mid-shelf and oceanic samples according to the Mann–Whitney test ($U = 42$, $p = 0.040$) but not the *t*-test (Table 1). Although inshore rates of N oxidation from urea-N and GLU-N were not included in statistical tests (since $n = 2$), high rates for both substrates were measured in some inshore samples.

Oxidation rates of N supplied as PUT, urea, or GLU were highly correlated with NH_4^+ oxidation (Spearman's $\rho > 0.80$,

Table 2. Regression parameters for model II (major axis) linear regressions. All pairwise comparisons used for regressions were significantly correlated according to Spearman's rank correlation test.

Explanatory*	Response*	Estimated slope (95% CI)	Slope $p^{\dagger}$	Estimated intercept (95% CI)	r^2	p	df
NH_4^+ ox.	PUT ox.	1.27 (0.97, 1.69)	0.001	−1.36 (−1.93, −0.95)	0.788	< 0.001	17
NH_4^+ ox.	Urea ox.	1.09 (0.63, 1.95)	0.001	−1.23 (−2.36, −0.62)	0.516	0.001	16
NH_4^+ ox.	GLU ox.	1.02 (0.61, 1.70)	0.003	−1.90 (−2.88, −1.32)	0.676	0.001	11
Thaum. 16S	WCA + WCB *amoA*	1.12 (0.93, 1.36)	0.001	−1.38 (−3.03, −0.05)	0.837	< 0.001	24
Thaum. 16S	*Nitrospina* 16S	0.78 (0.55, 1.08)	0.001	0.14 (−1.90, 1.72)	0.569	< 0.001	30

*All explanatory and response variables were log-transformed. "N oxidation rate" is abbreviated as "ox." and "thaumarchaeal" is abbreviated as "Thaum."
†The p value of the slope was estimated using 999 permutation tests.

$p < 0.001$ for all comparisons; Supporting Information Fig. S2). The slopes of linear regressions of PUT-, urea-, and GLU-N oxidation compared to NH_4^+ oxidation were not significantly different from 1 (Table 2; Fig. 2). Oxidation of PUT-N was consistently 5–10% of NH_4^+ oxidation across the data set (Supporting Information Table S1), reflected by the relatively small 95% confidence interval (CI) of the PUT-N oxidation vs. NH_4^+ oxidation regression slope (0.97–1.69, $p = 0.001$; Fig. 2a; Table 2), though some shelf-break and mid-shelf samples had higher oxidation rates of PUT-N relative to NH_4^+. In contrast, the CIs for regression slopes of urea-N (0.63–1.95, $p = 0.001$) and GLU-N oxidation vs. NH_4^+ oxidation (0.61–1.70, $p = 0.003$) were larger than that of the PUT-N oxidation vs. NH_4^+ oxidation regression (Table 2), reflecting the larger ranges of residuals in these regressions (Fig. 2b,c). Several oceanic and shelf-break samples had relatively high rates of urea-N oxidation compared to NH_4^+ (Fig. 2b; Supporting Information Table S1).

Potential oxidation rates of N supplied as DAE were typically lower than those of N supplied as DAP or PUT. PUT-N was typically oxidized most rapidly of the polyamines tested, though oxidation rates of N supplied as DAP and PUT were comparable in one of the samples (Marsh Landing, 2016; Fig. 3, Supporting Information Table S1). Oxidation rates of ARG-N were typically higher than GLU-N and comparable to PUT-N (Fig. 3). $^{15}NO_X$ formation from any of the organic N sources was negligible in filtered controls, as was formation of $^{15}N_2O$ when ^{15}N-labeled substrates were added directly to the denitrifier cultures used to convert NO_X to N_2O (data not shown).

Microbial communities

Bacterial 16S rRNA gene abundance was highest in surface or near-surface waters and decreased with depth (Fig. 4a) and was higher in inshore waters compared to shelf-break and ocean waters ($F_{2,32} = 19.1$, $p < 0.001$; Supporting Information Fig. S3a). Bacterial gene abundance ranged from 3.36×10^7 copies L^{-1} (Sta. 8, 500 m) to 9.48×10^{10} copies L^{-1} (Marsh Landing in 2013), with the three highest values at inshore stations.

Thaumarchaeota abundance (determined by 16S rRNA gene abundance or *amoA* abundance as either WCA or WCB) generally increased with depth (Fig. 4b,d,e), though the abundance of thaumarchaeal 16S rRNA genes in some shallow inshore samples was high (> 10^8 copies L^{-1}). Due to high 16S abundance both in shallow inshore waters and deeper shelfbreak/oceanic waters, Thaumarchaeota 16S rRNA gene abundance did not differ significantly between the three tested regions when data from all depths were included ($F_{2,29} = 1.4$, $p = 0.254$). The abundance of the WCA *amoA* clade was highest around 100–150 m at shelf-break and oceanic stations and decreased at greater depths (Fig. 4d). In contrast, the abundance of members of the WCB *amoA* clade increased with depth to a maximum below the photic zone (Fig. 4e). The sum of WCA and WCB *amoA* abundances was highly correlated with Thaumarchaeota 16S rRNA gene abundances for the entire sample set (Spearman's $\rho = 0.71$, $p < 0.001$; Fig. 5a), but this relationship differed with depth: WCA + WCB *amoA* abundance was substantially less than 16S gene abundance in most shallow samples (< 200 m) but was nearly equal to 16S gene abundance in deeper samples (Fig. 5). The linear regression between log-transformed thaumarchaeal 16S rRNA genes and the sum of the *amoA* ecotypes was highly significant ($r^2 = 0.837$, $p < 0.001$, df = 24; Fig. 5b; Table 2). The estimated regression slope was 1.12 (95% CI: 0.93, 1.36) and the 95% CI of the estimated intercept (−3.03, −0.05) did not include zero (Table 2). WCA and WCB *amoA* were not detected at inshore stations (though thaumarchaeal 16S rRNA gene abundances were high inshore; Fig. 4b, Supporting Information Table S1).

Nitrospina 16S rRNA genes were generally less abundant than thaumarchaeal genes (Fig. 4c; Supporting Information Table S1) but were highly correlated with Thaumarchaeota 16S rRNA genes (Spearman's $\rho = 0.617$, $p < 0.001$; Supporting Information Fig. S4). The linear regression of log-transformed *Nitrospina* and Thaumarchaeota 16S genes was significant ($r^2 = 0.57$, $p < 0.001$, df = 30), and the regression slope was 0.78 (95% CI: 0.55–1.08, $p = 0.001$; Table 2; Supporting Information Fig. S4b). Thaumarchaeal genes were about 10-fold more abundant than *Nitrospina* genes in most samples (Supporting Information Fig. S4, Table S1). The abundance of *Nitrospina* 16S rRNA genes did not differ significantly between the three tested regions when all depths were included ($F_{2,27} = 0.3$, $p = 0.721$; Supporting Information Fig. S3c).

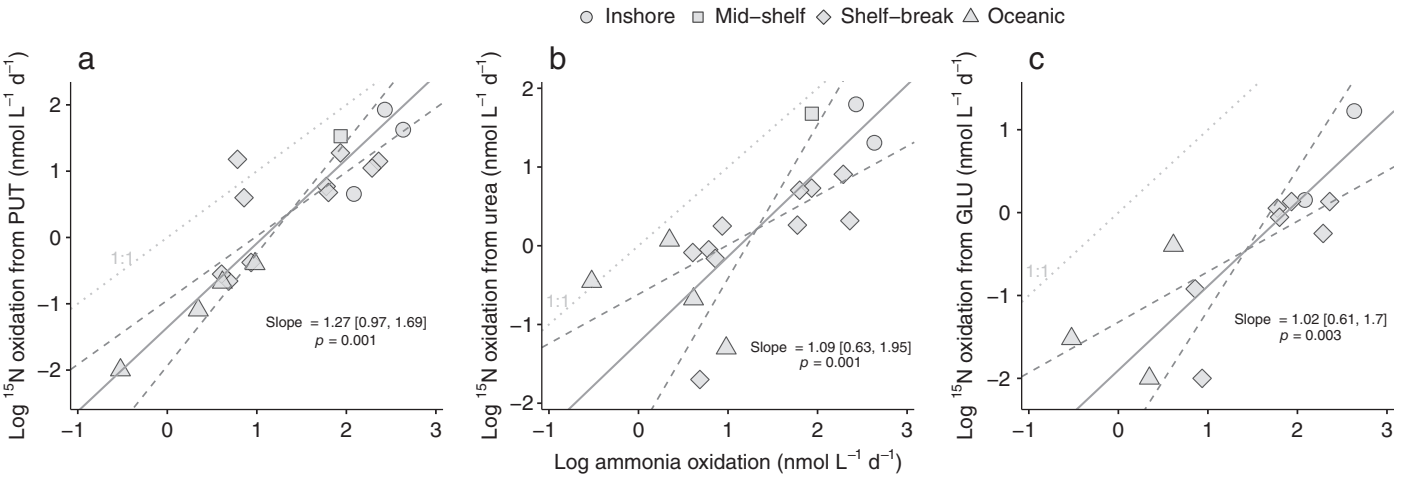

Fig. 2. Scatterplots of the oxidation rates of ^{15}N supplied as NH_4^+ vs. ^{15}N supplied as (**a**) putrescine, (**b**) urea, and (**c**) glutamate. Shapes indicate sampling region. Solid lines show the model II (major axis) regression line and the dashed lines indicate the 95% CI of the regression slope. The slope (including 95% CI bounds) and *p* value of the regression are indicated on the plot.

Discussion

Rapid oxidation of polyamine-N compared to amino acid-N and urea-N

Ammonia oxidation has been well characterized throughout the sea, and the rates measured here are consistent with general patterns of high rates near the base of the euphotic zone (e.g., Ward 1985; Santoro et al. 2010; Beman et al. 2012) and in near-shore/estuarine waters (e.g., Horrigan and Springer 1990; Bianchi et al. 1999; Ward 2005; Damashek and Francis 2018), and are comparable to previous measurements made in Georgia coastal waters (Tolar et al. 2016, 2017; Liu et al. 2018). Far less is known about oxidation of the N in DON, but recent demonstrations of thaumarchaeal oxidation of N supplied as urea and cyanate has stimulated interest in this aspect of marine DON cycling.

PUT-N was preferentially oxidized when compared to oxidation rates of N from urea or amino acids, though NH_4^+ oxidation typically outstripped oxidation of any form of DON we tested (Figs. 2, 3; Supporting Information Fig. S2). However, it is important to note that most DON oxidation rates presented here should be considered "potential" rates due to the elevated concentration of labeled substrate in amendments compared to the likely range of in situ concentrations. Although we were not able to measure concentrations of individual polyamines and amino acids in this set of samples, we have measured them in other samples from the SAB during previous studies (Lu et al. 2014; Liu et al. 2015). Concentrations of polyamines and DFAA in seawater are generally low: DFAA are typically tens to hundreds of nM (Lee and Bada 1977; Mopper and Lindroth 1982; Fuhrman 1990; Bronk and Glibert 1991; Keil and Kirchman 1999; Bradley et al. 2010), and polyamines are typically ~ 1 nM in coastal waters and even lower offshore, including the SAB (Nishibori et al. 2001*a*, 2003; Lu et al. 2014; Liu et al. 2015). Therefore, even 10–50 nM additions of polyamines or amino acids are beyond "tracer" level and may have affected microbial activity and N oxidation rates in our incubations. Since ammonia and urea concentrations in situ were higher, these can generally be considered "tracer" incubations and the resulting oxidation rates are more likely to represent in situ rates.

Our data suggest that PUT-N may be preferentially oxidized in the ocean compared to N supplied as shorter polyamines, urea, or amino acids, indicating that oxidation of N supplied as PUT may make a greater contribution to nitrification in coastal waters than oxidation of N from the other tested DON compounds. Comparing oxidation rates of N supplied as DAE, DAP, and PUT suggested that N oxidation rates may increase as the length of the polyamine-C skeleton increases from 2 (DAE) to 4 (PUT; Fig. 3). Unfortunately, the lack of commercially available ^{15}N-labeled polyamines of longer chain length precluded their use in these experiments, so we were unable to determine if this pattern holds for polyamines with longer C skeletons. Since we were unable to measure in situ polyamine concentrations, our calculated polyamine-N oxidation rates are likely different from in situ rates. However, the finding that PUT-N oxidation is higher than DAP- or DAE-N oxidation from the same waters is robust if concentrations of these polyamines are close to the range of individual polyamines previously measured in the SAB (Lu et al. 2014; Liu et al. 2015); note that neither DAE nor DAP were detected in these studies. For DAE-N or DAP-N oxidation rates to overtake those of PUT-N (given our measured isotope data and additions of ^{15}N), concentrations of these compounds would have to be orders of magnitude higher than the concentrations of other individual polyamines previously measured in the SAB (e.g., > 500 nM) while PUT concentrations remained low. Though possible, we believe this situation is unlikely to occur in the ocean. Clearly, though, our hypothesis of higher N oxidation rates with longer-chain polyamines should be tested by

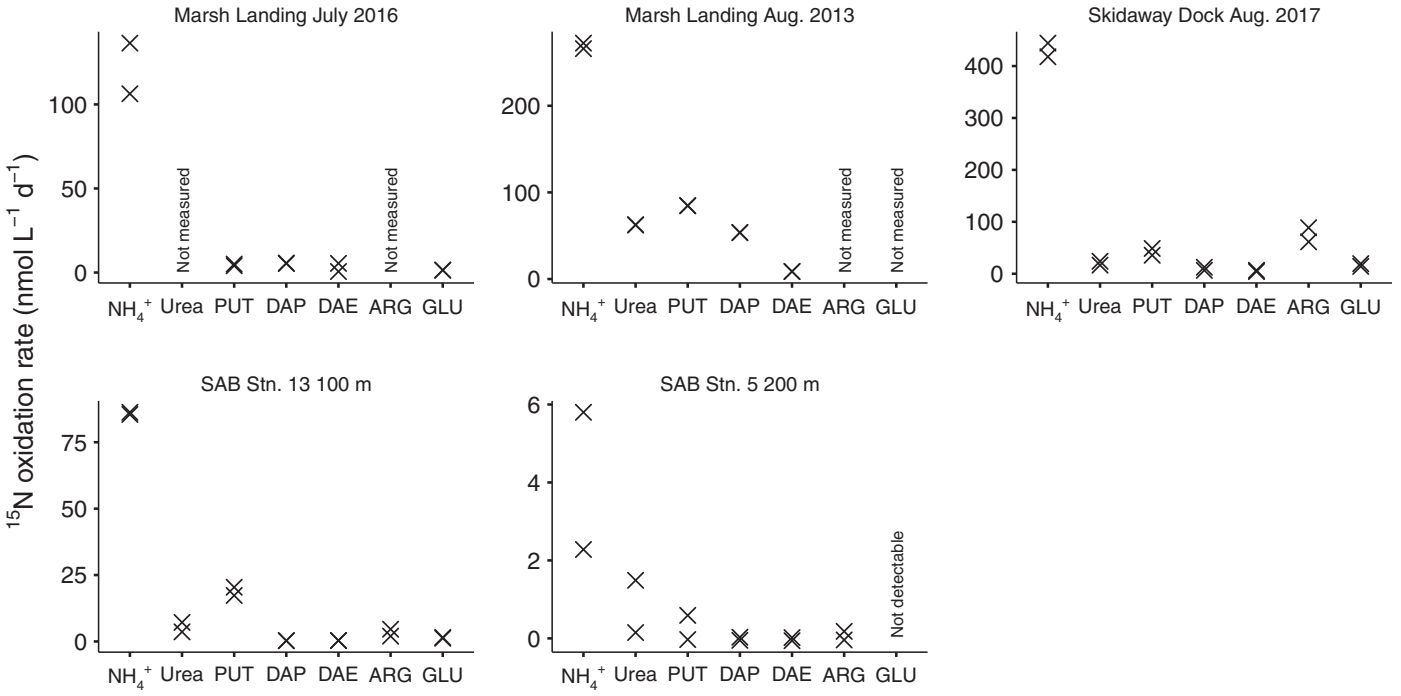

Fig. 3. Comparisons of oxidation rates of ^{15}N supplied as NH_4^+, urea, PUT, DAE, DAP, ARG, and GLU. Each point for each treatment indicates the value from one incubation; all treatments shown had duplicate incubations. Note the different *y*-axis scales.

measuring N oxidation rates and in situ concentrations of numerous polyamines throughout the ocean.

Of the amino acids we tested, oxidation of ARG-N was comparable to oxidation of PUT-N in some samples (though ARG-N oxidation was only measured in a small number of samples). Prior research has shown ARG-N is remineralized to NH_4^+ more rapidly than many other amino acids (Hollibaugh 1978; Goldman et al. 1987); our data suggest this rapid liberation of NH_4^+ may result in ARG contributing to nitrification to a greater degree than other amino acids. Oxidation of urea-N appears to have a greater contribution to nitrification in more oligotrophic waters, as oxidation rates of urea-N in deeper offshore waters of the SAB were equal to or greater than oxidation of PUT-N (Table 1; Fig. 2b; Supporting Information Table S1). However, oxidation of NH_4^+ was the dominant process in the majority of our samples.

Potential mechanisms of polyamine-N oxidation

The fact that oxidation of PUT-N was consistently faster than the oxidation of GLU-N (Fig. 3; Table 1) suggests either direct oxidation of PUT-N or surprisingly rapid regeneration of PUT-N to NH_4^+, since N supplied as GLU is rapidly regenerated to NH_4^+ compared to other amino acids (e.g., Crawford et al. 1974; Hollibaugh 1978; Amon et al. 2001). Given the structural similarity between primary amines and ammonia, it is tempting to speculate that Thaumarchaeota (the dominant marine ammonia oxidizer in these waters; Tolar et al. 2017; Liu et al. 2018) may be able to oxidize polyamine-N directly, leading to high rates of oxidation of PUT-N where Thaumarchaeota are abundant. However, we cannot rule out the possibility that N supplied as polyamines is regenerated as NH_4^+ more rapidly than N from other DON compounds, providing a significant source of NH_4^+ for Thaumarchaeota growing via canonical ammonia oxidation. The low C : N ratio of polyamines (e.g., 2 for PUT) compared to marine bacteria (e.g., 5–6; Goldman et al. 1987; Fukuda et al. 1998) suggests heterotrophs catabolizing polyamines could release a significant amount of polyamine-N as regenerated NH_4^+. The fact that oxidation rates of N from ARG (C : N = 1.5) were higher than GLU (C : N = 5; Fig. 3) may be an analogous case, as metabolism of a mole of ARG would liberate more NH_4^+ than a mole of GLU even though N remineralization rates from both are typically high (Hollibaugh 1978; Goldman et al. 1987). If remineralization coupled to NH_4^+ oxidation is the mechanism behind the observed oxidation rates of N supplied as polyamines, the high rates of N oxidation from PUT compared to urea and amino acids (Fig. 3; Table 1) suggests that remineralization of N from polyamines in the sea is surprisingly rapid, even compared to other more abundant forms of labile DON. Polyamines are indeed taken up rapidly and mineralized by heterotrophs in the SAB (Liu et al. 2015). The fact that heterotrophic assimilation of spermine and spermidine is typically faster than PUT (as judged by kinetic experiments with cultures and turnover rates in seawater; Tabor and Tabor 1966; Liu et al. 2015) suggests these two polyamines may also play a significant role in marine nitrification if polyamine-N oxidation is dependent on remineralization, particularly given high concentrations of intracellular spermidine in marine diatoms and cyanobacteria (Hamana and Matsuzaki 1985; Nishibori and Nishijima 2004; Liu et al. 2016).

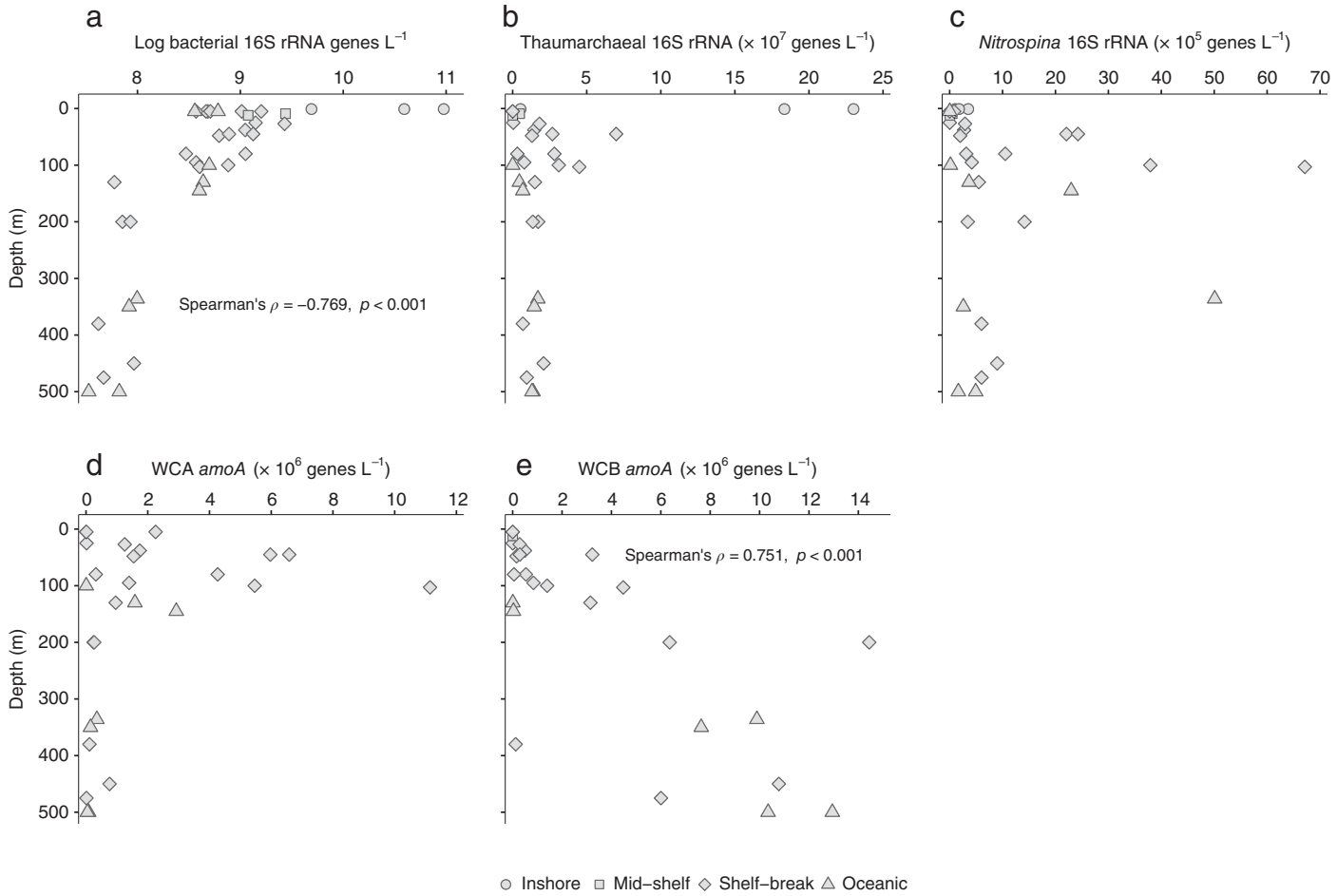

Fig. 4. Microbial abundance (qPCR) data from all samples, plotted by depth. Panels show the following genes: (**a**) bacterial 16S rRNA, (**b**) thaumarchaeal 16S rRNA, (**c**) *Nitrospina* 16S rRNA, (**d**) WCA *amoA*, and (**e**) WCB *amoA*. Shapes indicate the region sampled. When correlations between a single variable and depth were significant ($p < 0.05$), results of Spearman's rank correlation test are shown. Note the different *x*-axis scales.

At this point, we cannot distinguish between direct oxidation of polyamines by Thaumarchaeota or rapid remineralization polyamine-N followed by NH_4^+ oxidation. The fact that oxidation rates of N supplied as NH_4^+, urea, PUT, and GLU were all highly correlated (Fig. 2; Supporting Information Fig. S2) does not resolve this question, as these correlations predominantly reflect high-oxidation rates in coastal waters where both Thaumarchaeota and bacteria were abundant. Inshore waters of the SAB have high polyamine and amino acid turnover rates (Liu et al. 2015) and high bacterial production and respiration rates (Cai et al. 2003; Liu et al. 2015). Therefore, high-oxidation rates of N supplied as DON at inshore stations reflect the high-biogeochemical activity generally found in these waters regardless of whether the rapid N-oxidation is due to direct activity of abundant Thaumarchaeota or to the combined activity of heterotrophic remineralization and NH_4^+ oxidation. However, irrespective of the underlying mechanism, our data suggest that oxidation of polyamine-N may contribute to a significant fraction of total nitrification in waters where polyamine fluxes are high, such as decaying phytoplankton blooms or productive coastal waters (Lee and Jørgensen 1995; Nishibori et al. 2001*b*; Lu et al. 2014; Liu et al. 2015; Krempaska et al. 2018) and may therefore contribute significantly to DON oxidation in the coastal ocean.

In addition to steep gradients in environmental conditions and overall biogeochemical activity (e.g., Cai et al. 2003; Liu et al. 2015; Supporting Information Fig. S1), the phylogenetic composition of the dominant thaumarchaeal population changes from inshore to offshore waters in the SAB. WCA and WCB were abundant at the shelfbreak and in oceanic waters, while other thaumarchaeal clades are more abundant inshore and over the shelf (Supporting Information Fig. S3b,d,e; Liu et al. 2018; see below). Taking NH_4^+ oxidation rate as a proxy for thaumarchaeal activity, the consistent linear relationship between PUT-N and NH_4^+ oxidation rates in our combined data set (Fig. 2a; Table 2) suggests that PUT-N oxidation rates scale with thaumarchaeal *activity* across the SAB, regardless of the phylogenetic composition of the Thaumarchaeota population.

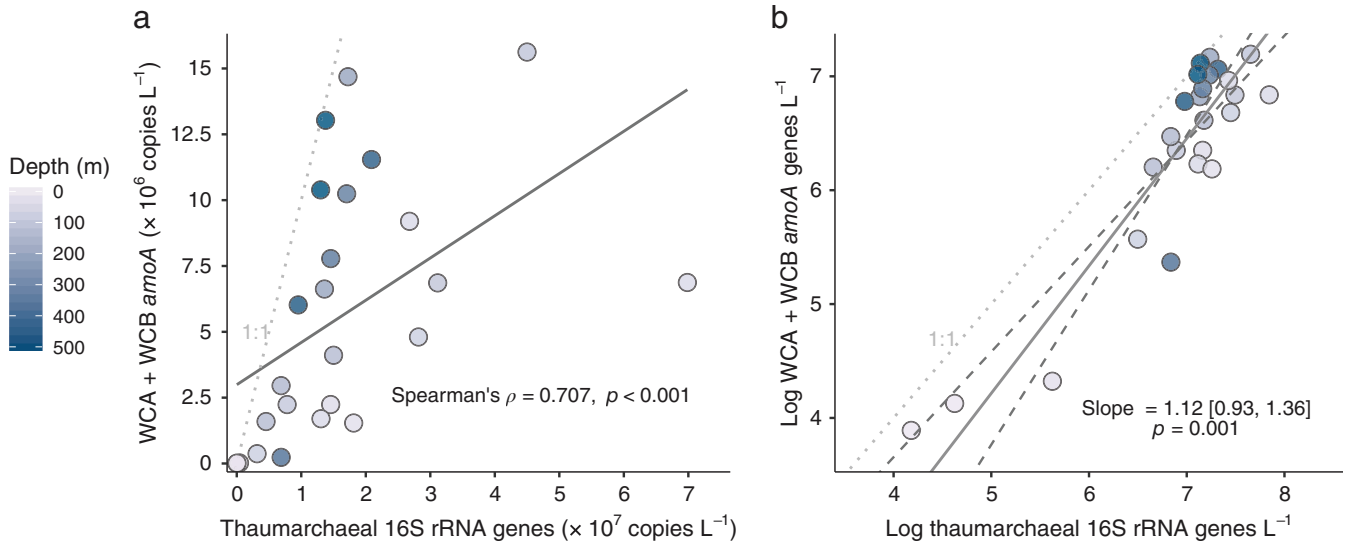

Fig. 5. Scatterplots of thaumarchaeal 16S rRNA gene abundance and the sum of WCA and WCB *amoA* gene abundance. Solid lines show a linear fit (type II major axis regression). Blue shading indicates depth. (**a**) Untransformed abundance data, with the results of Spearman's rank correlation test shown. (**b**) Log-transformed data. Dashed lines show the 95% CI of the regression slope. The estimated slope, 95% CI of the slope, and *p* value of a model II major axis regression are indicated.

Thaumarchaeal ecotypes in the SAB

Previous analyses of *amoA* clone libraries from the SAB suggested that members of the WCA clade dominate the thaumarchaeal community in shallower mid-shelf or shelf-break waters, whereas members of the WCB clade were more abundant in deeper waters (Liu et al. 2018). Since these data provided a picture of the overall thaumarchaeal diversity in the SAB, we focused on quantifying the WCA and WCB ecotypes, particularly around the shelf-break. Peak abundance of WCA was at 45–100 m near the shelf-break and slightly deeper (130–150 m) further offshore. WCB was most abundant in deeper (> 200 m) oceanic waters (Fig. 4e; Supporting Information Table S1).

Although the sum of WCA plus WCB abundance was highly correlated with the abundance of thaumarchaeal 16S rRNA genes in both shallow (< 200 m) and deep waters (Fig. 5), the greater abundance of 16S genes in shallow waters suggests that Thaumarchaeota ecotypes not detected by the WCA or WCB primer sets may be abundant there, given that all marine thaumarchaeal genomes sequenced to date have one copy of both the 16S rRNA gene and the *amoA* gene. Indeed, prior studies of thaumarchaeal diversity at inshore stations of the SAB have found clades other than WCA and WCB to be abundant at times (Hollibaugh et al. 2011, 2014; Liu et al. 2018), and studies comparing WCA and WCB abundance to "total" thaumarchaeal abundance in other coastal marine regions have found similar patterns (Smith et al. 2016; Damashek et al. 2017). In contrast, the sum of ecotypes accounted for the majority of Thaumarchaeota detected as 16S rRNA genes in deeper waters (Fig. 5), matching previous amplicon sequencing data from the SAB (Liu et al. 2018) as well as studies in other regions of the ocean (e.g., Francis et al. 2005; Kalanetra et al. 2009; Beman et al. 2010; Sintes et al. 2013; Santoro et al. 2017). Given the documented shifts in thaumarchaeal diversity from inshore to oceanic waters, our finding that PUT-N oxidation rates were a consistent fraction (~ 5–10%) of the NH_4^+ oxidation rates across the combined dataset suggests that, unlike urea oxidation (Alonso-Sáez et al. 2012; Qin et al. 2014; Bayer et al. 2016; Tolar et al. 2017; Carini et al. 2018), oxidation of PUT-N in the SAB is not directly related to thaumarchaeal diversity.

Nitrite-oxidizing bacteria in the SAB

Previous studies of the distributions of Thaumarchaeota and *Nitrospina* across the SAB found high abundance of both clades inshore (Liu et al. 2018). Our sampling, which was focused at deeper shelf-break and oceanic stations, captured a different distribution pattern: *Nitrospina* were not more abundant in our inshore samples (Supporting Information Fig. S3c), but co-occurrence of subsurface peaks of both clades at shelf-break and oceanic stations (Fig. 4b,c) drove a strong correlation between ammonia-oxidizing Thaumarchaeota and nitrite-oxidizing *Nitrospina* across our data set (Supporting Information Fig. S4). Similar co-occurring subsurface peaks were reported in the California Current, with Thaumarchaeota also outnumbering *Nitrospina* (Mincer et al. 2007; Santoro et al. 2010). Previous time series sampling in the SAB found lower abundance of *Nitrospina* than Thaumarchaeota in summer (Hollibaugh et al. 2014; Liu et al. 2018) due to more rapid growth of Thaumarchaeota at high temperature (Schaefer and Hollibaugh 2017). While the primer set used here does not capture all known nitrite oxidizers (e.g., *Nitrospira*, *Nitrobacter*, or *Nitrococcus*), previous analyses of 16S rRNA gene libraries from inshore stations (Amaral-Zettler et al. unpubl. data), of metatranscriptomes (Hollibaugh

et al. 2014), and of the composition of enrichment cultures raised from inshore SAB waters (Schaefer and Hollibaugh 2017) indicate that *Nitrospina*-like bacteria are the predominant nitrite oxidizers in this system, similar to other regions of the ocean (e.g., Füssel et al. 2012; Beman et al. 2013).

Conclusions

Previous studies of the contribution of DON-N to nitrification have largely focused on urea. Our data indicate that N from other DON compounds may be oxidized more rapidly than urea-N, though ammonia oxidation rates were generally higher than oxidation of N from any tested DON compound. In particular, N supplied as putrescine was oxidized at a significantly higher rate than N from urea and the amino acids we tested. It is unclear if marine Thaumarchaeota are able to use polyamine-N directly, or whether oxidation relies on rapid regeneration of polyamine-N to ammonium. Regardless of the mechanism, however, polyamine-N may contribute significantly to the production of nitrite and nitrate in the ocean. This work stresses the need to investigate the oxidation rates of N supplied as other DON compounds in the ocean, and begs the question whether marine Thaumarchaeota are capable of oxidizing polyamine-N directly.

References

Alonso-Sáez, L., and others. 2012. Role for urea in nitrification by polar marine Archaea. Proc. Natl. Acad. Sci. USA **109**: 17989–17994. doi:10.1073/pnas.1201914109

Amon, R. M. W., H. P. Fitznar, and R. Benner. 2001. Linkages among the bioreactivity, chemical composition, and diagenetic state of marine dissolved organic matter. Limnol. Oceanogr. **46**: 287–297. doi:10.4319/lo.2001.46.2.0287

Bayer, B., and others. 2016. Physiological and genomic characterization of two novel marine thaumarchaeal strains indicates niche differentiation. ISME J. **10**: 1051–1063. doi:10.1038/ismej.2015.200

Beman, J. M., B. N. Popp, and C. A. Francis. 2008. Molecular and biogeochemical evidence for ammonia oxidation by marine Crenarchaeota in the Gulf of California. ISME J. **2**: 429–441. doi:10.1038/ismej.2007.118

Beman, J. M., R. Sachdeva, and J. A. Fuhrman. 2010. Population ecology of nitrifying archaea and bacteria in the Southern California Bight. Environ. Microbiol. **12**: 1282–1292. doi:10.1111/j.1462-2920.2010.02172.x

Beman, J. M., and others. 2011. Global declines in oceanic nitrification rates as a consequence of ocean acidification. Proc. Natl. Acad. Sci. USA **108**: 208–213. doi:10.1073/pnas.1011053108

Beman, J. M., B. N. Popp, and S. E. Alford. 2012. Quantification of ammonia oxidation rates and ammonia-oxidizing archaea and bacteria at high resolution in the Gulf of California and eastern tropical North Pacific Ocean. Limnol. Oceanogr. **57**: 711–726. doi:10.4319/lo.2012.57.3.0711

Beman, J. M., J. L. Shih, and B. N. Popp. 2013. Nitrite oxidation in the upper water column and oxygen minimum zone of the eastern tropical North Pacific Ocean. ISME J. **7**: 2192–2205. doi:10.1038/ismej.2013.96

Bianchi, M., C. Fosset, and P. Conan. 1999. Nitrification rates in the NW Mediterranean Sea. Aquat. Microb. Ecol. **17**: 267–278. doi:10.3354/ame017267

Bradley, P. B., M. P. Sanderson, M. E. Frischer, J. Brofft, M. G. Booth, L. J. Kerkhof, and D. A. Bronk. 2010. Inorganic and organic nitrogen uptake by phytoplankton and heterotrophic bacteria in the stratified Mid-Atlantic Bight. Estuar. Coast. Shelf Sci. **88**: 429–441. doi:10.1016/j.ecss.2010.02.001

Bronk, D. A., and P. M. Glibert. 1991. A ^{15}N tracer method for the measurement of dissolved organic nitrogen release by phytoplankton. Mar. Ecol. Prog. Ser. **77**: 171–182. doi:10.3354/meps077171

Cai, W. J., Z. A. Wang, and Y. Wang. 2003. The role of marsh-dominated heterotrophic continental margins in transport of CO_2 between the atmosphere, the land-sea interface and the ocean. Geophys. Res. Lett. **30**: 1849. doi:10.1029/2003GL017633

Carini, P., C. L. DuPont, and A. E. Santoro. 2018. Patterns of thaumarchaeal gene expression in culture and diverse marine environments. Environ. Microbiol. **20**: 2112–2124. doi:10.1111/1462-2920.14107

Casciotti, K. L., D. M. Sigman, M. G. Hastings, J. K. Böhlke, and A. Hilkert. 2002. Measurement of the oxygen isotopic composition of nitrate in seawater and freshwater using the denitrifier method. Anal. Chem. **74**: 4905–4912. doi:10.1021/ac020113w

Connelly, T. L., S. E. Baer, J. T. Cooper, D. A. Bronk, and B. Wawrik. 2014. Urea uptake and carbon fixation by marine pelagic bacteria and archaea during the Arctic summer and winter seasons. Appl. Environ. Microbiol. **80**: 6013–6022. doi:10.1128/AEM.01431-14

Crawford, C. C., J. E. Hobbie, and K. L. Webb. 1974. The utilization of dissolved free amino acids by estuarine microorganisms. Ecology **55**: 551–563. doi:10.2307/1935146

Damashek, J., K. L. Casciotti, and C. A. Francis. 2016. Variable nitrification rates across environmental gradients in turbid, nutrient-rich estuary waters of San Francisco Bay. Estuaries Coast. **39**: 1050–1071. doi:10.1007/s12237-016-0071-7

Damashek, J., K. P. Pettie, Z. W. Brown, M. M. Mills, K. R. Arrigo, and C. A. Francis. 2017. Regional patterns in ammonia-oxidizing communities throughout Chukchi Sea waters from the Bering Strait to the Beaufort Sea. Aquat. Microb. Ecol. **79**: 273–286. doi:10.3354/ame01834

Damashek, J., and C. A. Francis. 2018. Microbial nitrogen cycling in estuaries: From genes to ecosystems processes. Estuaries Coast. **41**: 626–660. doi:10.1007/s12237-017-0306-2

de Mendiburu, F. 2015. Agricolae: Statistical procedures for agricultural research. R package version 1.2-3. Available from http://CRAN.R-project.org/package=agricolae. Last accessed 26 Sep 2018

Edwards, S. M. 2018. lemon: Freshing up your "ggplot2" plots. R package version 0.3.3. Available from https://CRAN.R-project.org/package=lemon. Last accessed 2 Aug 2018

Ferrari, V. C., and J. T. Hollibaugh. 1999. Distribution of microbial assemblages in the Central Arctic Ocean Basin studied by PCR/DGGE: Analysis of a large data set. Hydrobiologia **401**: 55–68. doi:10.1023/A:1003773907789

Francis, C. A., K. J. Roberts, J. M. Beman, A. E. Santoro, and B. B. Oakley. 2005. Ubiquity and diversity of ammonia-oxidizing archaea in water columns and sediments of the ocean. Proc. Natl. Acad. Sci. USA **102**: 14683–14688. doi:10.1073/pnas.0506625102

Fuhrman, J. 1990. Dissolved free amino acid cycling in an estuarine outflow plume. Mar. Ecol. Prog. Ser. **66**: 197–203. doi:10.3354/meps066197

Fukuda, R., H. Ogawa, T. Nagata, and I. Koike. 1998. Direct determination of carbon and nitrogen contents of natural bacterial assemblages in marine environments. Appl. Environ. Microbiol. **64**: 3352–3358.

Füssel, J., P. Lam, G. Lavik, M. M. Jensen, M. Holtappels, M. Günter, and M. M. M. Kuypers. 2012. Nitrite oxidation in the Namibian oxygen minimum zone. ISME J. **6**: 1200–1209. doi:10.1038/ismej.2011.178

Goldman, J. C., D. A. Caron, and M. R. Dennett. 1987. Regulation of gross growth efficiency and ammonium regeneration in bacteria by substrate C:N ratio. Limnol. Oceanogr. **32**: 1239–1252. doi:10.4319/lo.1987.32.6.1239

Hamana, K., and S. Matsuzaki. 1985. Further study on polyamines in primitive unicellular eukaryotic algae. J. Biochem. **97**: 1311–1315. doi:10.1093/oxfordjournals.jbchem.a135182

Höfle, M. G. 1984. Degradation of putrescine and cadaverine in seawater cultures by marine bacteria. Appl. Environ. Microbiol. **47**: 843–849.

Hollibaugh, J. T. 1978. Nitrogen regeneration during the degradation of several amino acids by plankton communities collected near Halifax, Nova Scotia, Canada. Mar. Biol. **45**: 191–201. doi:10.1007/BF00390601

Hollibaugh, J. T., S. Gifford, S. Sharma, N. Bano, and M. A. Moran. 2011. Metatranscriptomic analysis of ammonia-oxidizing organisms in an estuarine bacterioplankton assemblage. ISME J. **5**: 866–878. doi:10.1038/ismej.2010.172

Hollibaugh, J. T., S. M. Gifford, M. A. Moran, M. J. Ross, S. Sharma, and B. B. Tolar. 2014. Seasonal variation in the metratranscriptomes of a Thaumarchaeota population from SE USA coastal waters. ISME J. **8**: 685–698. doi:10.1038/ismej.2013.171

Horrigan, S. G., and A. L. Springer. 1990. Oceanic and estuarine ammonium oxidation: Effects of light. Limnol. Oceanogr. **35**: 479–482. doi:10.4319/lo.1990.35.2.0479

Iacomino, G., G. Picariello, and L. D'Agostino. 2012. DNA and nuclear aggregates of polyamines. Biochim. Biophys. Acta **1823**: 1745–1755. doi:10.1016/j.bbamcr.2012.05.033

Kalanetra, K. M., N. Bano, and J. T. Hollibaugh. 2009. Ammonia-oxidizing *Archaea* in the Arctic Ocean and Antarctic coastal waters. Environ. Microbiol. **11**: 2434–2445. doi:10.1111/j.1462-2920.2009.01974.x

Keil, R. G., and D. L. Kirchman. 1999. Utilization of dissolved protein and amino acids in the northern Sargasso Sea. Aquat. Microb. Ecol. **18**: 293–300. doi:10.3354/ame018293

Krempaska, N., K. Horňák, and J. Pernthaler. 2018. Spatiotemporal distribution and microbial assimilation of polyamines in a mesotrophic lake. Limnol. Oceanogr. **63**: 816–832. doi:10.1002/lno.10672

Kröger, N., R. Deutzmann, C. Bergsdorf, and M. Sumper. 2000. Species-specific polyamines from diatoms control silica morphology. Proc. Natl. Acad. Sci. USA **97**: 14133–14138. doi:10.1073/pnas.260496497

Lee, C., and J. L. Bada. 1977. Dissolved amino acids in the equatorial Pacific, the Sargasso Sea, and Biscayne Bay. Limnol. Oceanogr. **22**: 502–510. doi:10.4319/lo.1977.22.3.0502

Lee, C., and N. O. G. Jørgensen. 1995. Seasonal cycling of putrescine and amino acids in relation to biological production in a stratified coastal salt pond. Biogeochemistry **29**: 131–157. doi:10.1007/BF00000229

Legendre, P. 2018. lmodel2: Model II regression. R package version 1.7-3. Available from https://CRAN.R-project.org/package=lmodel2. Last accessed 3 Oct 2018

Legendre, P., and L. Legendre. 2012. Numerical ecology, 3rd ed. Elsevier.

Liu, Q., X. Lu, B. B. Tolar, X. Mou, and J. T. Hollibaugh. 2015. Concentrations, turnover rates and fluxes of polyamines in coastal waters of the South Atlantic Bight. Biogeochemistry **123**: 117–133. doi:10.1007/s10533-014-0056-1

Liu, Q., N. Nishibori, I. Imai, and J. T. Hollibaugh. 2016. Response of polyamine pools in marine phytoplankton to nutrient limitation and variation in temperature and salinity. Mar. Ecol. Prog. Ser. **544**: 93–105. doi:10.3354/meps11583

Liu, Q., B. B. Tolar, M. J. Ross, J. B. Cheek, C. M. Sweeney, N. J. Wallsgrove, B. N. Popp, and J. T. Hollibaugh. 2018. Light and temperature control the seasonal distribution of thaumarchaeota in the South Atlantic bight. ISME J. **12**: 1473–1485. doi:10.1038/s41396-018-0066-4

Lu, X., L. Zou, C. Clevinger, Q. Liu, J. T. Hollibaugh, and X. Mou. 2014. Temporal dynamics and depth variations of dissolved free amino acids and polyamines in coastal seawater determined by high-performance liquid chromatography. Mar. Chem. **163**: 36–44. doi:10.1016/j.marchem.2014.04.004

Lu, X., S. Sun, J. T. Hollibaugh, and X. Mou. 2015. Identification of polyamine-responsive bacterioplankton taxa in South Atlantic Bight. Environ. Microbiol. Rep. **7**: 831–838. doi:10.1111/1758-2229.12311

McIlvin, M. R., and K. L. Casciotti. 2011. Technical updates to the bacterial method for nitrate isotopic analyses. Anal. Chem. **83**: 1850–1856. doi:10.1021/ac1028984

Mincer, T. J., M. J. Church, L. T. Taylor, C. Preston, D. M. Karl, and E. F. DeLong. 2007. Quantitative distribution of presumptive archaeal and bacterial nitrifiers in Monterey Bay and the North Pacific Subtropical Gyre. Environ. Microbiol. **9**: 1162–1175. doi:10.1111/j.1462-2920.2007.01239.x

Mopper, K., and P. Lindroth. 1982. Diel and depth variations in dissolved free amino acids and ammonium in the Baltic Sea determined by shipboard HPLC analysis. Limnol. Oceanogr. **27**: 336–347. doi:10.4319/lo.1982.27.2.0336

Mosier, A. C., and C. A. Francis. 2011. Determining the distribution of marine and coastal ammonia-oxidizing archaea and bacteria using a quantitative approach, p. 205–221. *In* M. G. Klotz and L. Y. Stein [eds.], Methods in enzymology: Research on nitrification and related processes, part a. Elsevier.

Mou, X., M. Vila-Costa, S. Sun, W. Zhao, S. Sharma, and M. A. Moran. 2011. Metatranscriptomic signature of exogenous polyamine utilization by coastal bacterioplankton. Environ. Microbiol. Rep. **3**: 798–806. doi:10.1111/j.1758-2229.2011.00289.x

Mou, X., J. Jacob, X. Lu, M. Vila-Costa, L. K. Chan, S. Sharma, and Y. Q. Zhang. 2015. Bromodeoxyuridine labelling and fluorescence-activated cell sorting of polyamine-transforming bacterioplankton in coastal seawater. Environ. Microbiol. **17**: 876–888. doi:10.1111/1462-2920.12550

Mulvenna, P. F., and G. Savidge. 1992. A modified manual method for the determination of urea in seawater using diacetylmonoxime reagent. Estuar. Coast. Shelf Sci. **34**: 429–438. doi:10.1016/S0272-7714(05)80115-5

Nishibori, N., A. Nishii, and H. Takayama. 2001*a*. Detection of free polyamine in coastal seawater using ion exchange chromatography. ICES J. Mar. Sci. **58**: 1201–1207. doi:10.1006/jmsc.2001.1115

Nishibori, N., A. Yuasa, M. Sakai, S. Fujihara, and S. Nishio. 2001*b*. Free polyamine concentrations in coastal seawater during phytoplankton bloom. Fish. Sci. **67**: 79–83. doi:10.1046/j.1444-2906.2001.00202.x

Nishibori, N., Y. Matuyama, T. Uchida, T. Moriyama, Y. Ogita, M. Oda, and H. Hirota. 2003. Spatial and temporal variations in free polyamine distributions in Uranouchi Inlet, Japan. Mar. Chem. **82**: 307–314. doi:10.1016/S0304-4203(03)00076-8

Nishibori, N., and T. Nishijima. 2004. Changes in polyamine levels during growth of a red-tide causing phytoplankton *Chattonella antiqua* (Raphidophyceae). Eur. J. Phycol. **39**: 51–55. doi:10.1080/0967026031000163667 7

Palatinszky, M., and others. 2015. Cyanate as an energy source for nitrifiers. Nature **524**: 105–108. doi:10.1038/nature14856

Pante, E., and B. Simon-Bouhet. 2013. marmap: A package for importing, plotting and analyzing bathymetric and topographic data in R. PLoS One **8**: e73051. doi:10.1371/journal.pone.0073051

Poretsky, R. S., S. Sun, X. Mou, and M. A. Moran. 2010. Transporter genes expressed by coastal bacterioplankton in response to dissolved organic carbon. Environ. Microbiol. **12**: 616–627. doi:10.1111/j.1462-2920.2009.02102.x

Qin, W., and others. 2014. Marine ammonia-oxidizing archaeal isolates display obligate mixotrophy and wide ecotypic variation. Proc. Natl. Acad. Sci. USA **111**: 12504–12509. doi:10.1073/pnas.1324115111

Qin, W., and others. 2017. *Nitrosopumilus maritimus* gen. Nov., sp. nov., *Nitrosopumilus comalaminigenes* sp. nov., *Nitrosopumilus oxyclinae* sp. nov., and *Nitrosopumilus ureiphilus* sp. nov., four marine ammonia-oxidizing archaea of the phylum *Thaumarchaeota*. Int. J. Syst. Evol. Microbiol. **67**: 5067–5079. doi:10.1099/ijsem.0.002416

R Core Team. 2015. R: A language and environment for statistical computing. R Foundation for Statistical Computing. Available from http://www.R-project.org/. Last accessed 3 Oct 2018

Rahmatullah, M., and T. R. C. Boyde. 1980. Improvements in the determination of urea using diacetyl monoxime; methods with and without deproteinisation. Clin. Chim. Acta **107**: 3–9. doi:10.1016/0009-8981(80)90407-6

Santoro, A. E., K. L. Casciotti, and C. A. Francis. 2010. Activity, abundance and diversity of nitrifying archaea and bacteria in the Central California Current. Environ. Microbiol. **12**: 1989–2006. doi:10.1111/j.1462-2920.2010.02205.x

Santoro, A. E., M. A. Saito, T. J. Goepfert, C. H. Lamborg, C. L. Dupont, and G. R. DiTullio. 2017. Thaumarchaeal ecotype distributions across the equatorial Pacific Ocean and their potential roles in nitrification and sinking flux attenuation. Limnol. Oceanogr. **62**: 1984–2003. doi:10.1002/lno.10547

Sauder, L. A., K. Engel, C. C. Lo, P. Chain, and J. D. Neufeld. 2018. "*Candidatus* Nitrosotenuis aquarius," an ammonia-oxidizing archaeon from a freshwater aquarium biofilter. Appl. Environ. Microbiol. **84**: e01430–e01418. doi:10.1128/AEM.01430-18

Schaefer, S. C., and J. T. Hollibaugh. 2017. Temperature decouples ammonium and nitrite oxidation in coastal waters. Environ. Sci. Technol. **51**: 3157–3164. doi:10.1021/acs.est.6b03483

Sigman, D. M., K. L. Casciotti, M. Andreani, C. Barford, M. Galanter, and J. K. Böhlke. 2001. A bacterial method for the nitrogen isotopic analysis of nitrate in seawater and freshwater. Anal. Chem. **73**: 4145–4153. doi:10.1021/ac010088e

Sintes, E., K. Bergauer, D. De Corte, T. Yokokawa, and G. J. Herndl. 2013. Archaeal *amo*A gene diversity points to distinct biogeography of ammonia-oxidizing *Crenarchaeota* in the ocean. Environ. Microbiol. **15**: 1647–1658. doi:10.1111/j.1462-2920.2012.02801.x

Sipler, R. E., and D. A. Bronk. 2015. Dynamics of dissolved organic nitrogen, p. 127–232. *In* D. A. Hansell and C. A. Carlson [eds.], Biogeochemistry of marine dissolved organic matter. Elsevier.

Smith, J. M., J. Damashek, F. P. Chavez, and C. A. Francis. 2016. Factors influencing nitrification rates and the abundance and transcriptional activity of ammonia-oxidizing microorganisms in the dark Northeast Pacific Ocean. Limnol. Oceanogr. **61**: 596–609. doi:10.1002/lno.10235

Solórzano, L. 1969. Determination of ammonia in natural waters by the phenolhypochlorite method. Limnol. Oceanogr. **14**: 799–801. doi:10.4319/lo.1969.14.5.0799

Tabor, C. W., and H. Tabor. 1966. Transport systems for 1,4-diaminobutane, spermidine, and spermine in *Escherichia coli*. J. Biol. Chem. **241**: 3714–3723.

Tabor, C. W., and H. Tabor. 1985. Polyamines in microorganisms. Microbiol. Rev. **49**: 81–99.

Tolar, B. B., G. M. King, and J. T. Hollibaugh. 2013. An analysis of Thaumarchaeota populations from the Northern Gulf of Mexico. Front. Microbiol. **4**: 72. doi:10.3389/fmicb.2013.00072

Tolar, B. B., L. C. Powers, W. L. Miller, N. J. Wallsgrove, B. N. Popp, and J. T. Hollibaugh. 2016. Ammonia oxidation in the ocean can be inhibited by nanomolar concentrations of hydrogen peroxide. Front. Mar. Sci. **3**: 237. doi:10.3389/fmars.2016.00237

Tolar, B. B., N. J. Wallsgrove, B. N. Popp, and J. T. Hollibaugh. 2017. Oxidation of urea-derived nitrogen by thaumarchaeota-dominated marine nitrifying communities. Environ. Microbiol. **19**: 4838–4850. doi:10.1111/1462-2920.13457

Tourna, M., and others. 2011. *Nitrososphaera viennensis*, an ammonia oxidizing archaeon from soil. Proc. Natl. Acad. Sci. USA **108**: 8420–8425. doi:10.1073/pnas.1013488108

Ward, B. B. 1985. Light and substrate concentration relationships with marine ammonium assimilation and oxidation rates. Mar. Chem. **16**: 301–316. doi:10.1016/0304-4203(85)90052-0

Ward, B. B. 2005. Temporal variability in nitrification rates and related biogeochemical factors in Monterey Bay, California, USA. Mar. Ecol. Prog. Ser. **292**: 97–109. doi:10.3354/meps292097

Whitby, H., J. T. Hollibaugh, and C. M. G. van den Berg. 2017. Chemical speciation of copper in a salt marsh estuary and bioavailability to Thaumarchaeota. Front. Mar. Sci. **4**: 178. doi:10.3389/fmars.2017.00178

Wickham, H. 2009. ggplot2: Elegant graphics for data analysis. Springer.

Wilkerson, F. P., R. C. Dugdale, A. E. Parker, S. B. Blaser, and A. Pimenta. 2015. Nutrient uptake and primary productivity in an urban estuary: Using rate measurements to evaluate phytoplankton response to different hydrological and nutrient conditions. Aquat. Ecol. **49**: 211–233. doi:10.1007/s10452-015-9516-5

Yakimov, M. M., and others. 2011. Contribution of crenarchaeal autotrophic ammonia oxidizers to the dark primary production in Tyrrhenian deep waters (Central Mediterranean Sea). ISME J. **5**: 945–961. doi:10.1038/ismej.2010.197

Acknowledgments

We thank the captain and crew of the R/V *Savannah*, the staff of the University of Georgia Marine Institute at Sapelo Island, the GCE-LTER field crew, Leanne Powers, and Bryndan Durham for assistance with sample collection. Sarah Blaser, Frances Wilkerson, and Dick Dugdale provided nutrient concentration data. Whitney Ko assisted with $^{15}N\text{-}NO_X$ measurements. Meredith Ross assisted with DNA extractions from 2011 samples. Comments from three anonymous reviewers greatly improved the manuscript. This work was funded by NSF OCE grants 1538677 (to JTH), 1537995 (to BNP), and 12-37140 (to the GCE-LTER). This is contribution number 1072 from the UGA Marine Institute and SOEST contribution number 10523.

Conflict of Interest

None declared.

Submitted 2 August 2018
Revised 4 October 2018
Accepted 02 November 2018

Associate editor: Maren Voss